ORIGINAL PAPER

Influence of Prototropic Reactions on the Absorption and Fluorescence Spectra of Methyl p-dimethylaminobenzoate and Its Two Ortho Derivatives

M. Józefowicz · M. Aleksiejew · A. V. Abramov · S. Ling · M. Gutowski · J. Heldt · J. R. Heldt

Abstract The influence of prototropic reactions on the spectral characteristics of methyl p-dimethylaminobenzoate (I) and its o-methoxy (II) and o-hydroxy (III) derivatives has been studied using steady-state spectroscopic technique and quantum-chemical calculations. This study concerns the solvent-induced shift of the absorption, locally excited (LE) and intramolecular charge transfer (ICT) fluorescence bands in the neat tetrahydrofuran (THF) and its hydrochloric acid solutions at different HCl concentrations. On the basis of the experimental results and quantum-chemical calculations, it was shown that in a hydrochloric acid solution the studied molecules exist as a mixture of neutral, mono-, and dicationic forms. Additionally, the results of spectroscopic measurements were used to calculate, according to the Benesi-Hildebrand method, the equilibrium constants of protropic reactions in the ground, S_0, and excited, S_1, states. Our findings predestine molecules I and II to be used as acid fluorescence probes in a region of 0–2.5 M of [H$^+$] concentrations.

Keywords Methyl p-dimethylaminobenzoate · Absorption and emission spectra · Quantum-chemical calculations · Fluorescence quenching

Dedicated to Professor Michael Kasha on the occasion of his 90-th birthday

M. Józefowicz (✉) · M. Aleksiejew · J. Heldt · J. R. Heldt
Institute of Experimental Physics, University of Gdańsk,
ul. Wita Stwosza 57,
80-952 Gdańsk, Poland
e-mail: fizmj@univ.gda.pl

A. V. Abramov · S. Ling · M. Gutowski
Department of Chemistry, School of Engineering and Physical Sciences, Heriot-Watt University,
Edinburgh EH14 4AS, UK

Introduction

In a series of papers [1–10], it has been shown that methyl p-dimethylaminobenzoate (I) and its ortho derivatives (–OCH$_3$ (II) and –OH (III)) exhibit dual fluorescence in polar solvents, i.e., the normal (locally excited (LE)) fluorescence $S_1(LE) \rightarrow S_0(LE)$ and the twisted intramolecular charge transfer fluorescence $S_1(ICT) \rightarrow S_0(ICT)$. The two emission modes originate from independent electronic transitions of planar and non-planar spatial conformers, in which the plane of the electron donor substituent (–NMe$_2$) is parallel or perpendicular to the plane of benzene skeleton. In polar solvents, the initially populated LE state reacts further to produce a stable twisted intramolecular charge transfer (TICT) state, which gives rise to a second (long-wavelength) fluorescence band. This conformation change facilitates an electron transfer process from the donor (–NMe$_2$) to the methyl benzoate skeleton (charge accepting moiety). The appearance of two or three radiative modes in the fluorescence spectrum, associated with a definite isomeric or tautomeric form of the excited molecule, has been confirmed by picosecond transient absorption measurements [3] and steady-state absorption and fluorescence studies [1, 2, 4–9] in solvents of different polarity.

The isomeric or tautomeric spatial form of the parent molecule possesses a higher electric dipole moment and emits fluorescence quanta of lower energy. Its photophysical parameters, e.g., transition energy E_{00}, fluorescence rate constant $k_F = Q_F/\tau_F$ (fluorescence quantum yield Q_F and lifetime τ_F) differ significantly from that of the parent molecule [2, 4, 8, 9]. The efficiencies of the photoinduced intramolecular reactions i.e., the intramolecular charge transfer $S_1(LE) \rightarrow S_1(ICT)$ or the intramolecular proton transfer $S_1(LE) \rightarrow S_1(IPT)$ are determined by the dipole-dipole solute-solvent interactions, as well as they can be

influenced by external factors such as a short range anisotropic interaction (hydrogen bonding) with one or more solvent molecules causing changes in the absorption and fluorescence spectra (changes in fluorescence yield, the shape of fluorescence emission spectra, position of fluorescence maxima) [10]. Ghosh and co-workers [11] have shown that a chemical reaction of a H^+ ion with the $-NMe_2$ substitutent changes the C–N bond length and as a consequence makes torsional motions to be more complex. As a result of that the dialkylamino group forms a specific complex, which severely polarises one end of the molecule.

Since our earlier papers [7, 8] concern spectroscopic studies of methyl p-dimethylaminobenzoate and its ortho derivatives, it is very interesting to study the influence of the H^+ ion concentration on the steady-state absorption and fluorescence spectra of methyl p-dimethylaminobenzoate (I) and its o-methoxy (II), o-hydroxy (III) derivatives. The chemical structures of compounds of interest are given in Scheme 1. The results of spectroscopic studies were compared with results of our quantum-chemical calculations.

Methods

Steady-state absorption and fluorescence measurements at room temperature were carried out using a computer-controlled Shimadzu UV-2401 PC Spectrophotometer and Shimadzu RF-5301 PC spectrofluorometer with a 3 nm bandwidth in excitation and 5 nm bandwidth in emission. Fluorescence measurements were carried out using the triangular cuvette with frontal excitation to minimize the effect of reabsorption. The emission was observed perpendicular to the direction of the exciting beam. Thus the errors due to fluorescence reabsorption were reduced in a way that mathematical corrections were superfluous. The luminescence spectra have been corrected for the spectral response of the photomultiplier Hamamatsu R-928. In the conversion between wavelength and wavenumber representation of the absorption and emission spectra the reweighing intensities factor has been taken into account [12].

The solvents tetrahydrofuran (THF) and hydrochloric acid (HCl) were purchased from Aldrich Chemical Co as highest grade commercially available. Additionally, solvents were checked in both steady-state and time-resolved fluorescence apparatuses for lack of fluorescent impurities in the wavelength ranges of interest. The concentration of molecules in the solutions was about 10^{-4} M.

All calculations concerning absorption spectra of neutral and protonated molecules (see Scheme 1) were performed using the Gaussian 09 code [13]. The first problem that we addressed was identification of the most stable conformers. We used the Systematic Screening of Conformers (SSC) software [14, 15] to generate a library of conformers for each

molecule. For the first four molecules (I, IA-B, and II) all rotational degrees of freedom were considered at this stage. Next, we recognized that the contribution from methyl groups to the overall stability of molecules is relatively small and can be decoupled from contributions associated with other rotational degrees of freedom. Thus for the remaining five molecules (IIA-B, III, IIIA-B) the rotational degrees of freedom of methyl groups were not considered when creating initial libraries of conformers with SSC. The stability of each conformer was initially determined in the course of geometry optimization with the B3LYP exchange-correlation functional [16, 17] and the 6-31G* basis set [18], including geometrical relaxation of all methyl groups. A typical library created with SSC contained a few hundreds of conformers and the B3LYP/6-31G* optimization led to a few tens of distinct local minima, see Table 1. For these local minima all meaningful conformers derived from rotations of methyl groups were considered. At the second stage, the structures of the most stable conformers of each molecule were further refined at the B3LYP/6-311G** level [19]. The number n of conformers included at the second stage of search was selected in this way that the $(n+1)$-th conformer was less stable than the n-th conformer by at least 2 kcal/mol. The details of our two-step procedure are summarized in Table 1. For example, for the diprotonated methyl o-hydroxy p-dimethylaminobenzoate (IIIB) the SSC software created 218 initial conformers and the B3LYP/6-31G* prescreening step led to 30 distinct conformers. The two most stable conformers spanned a narrow range of 0.2 kcal/mol and the third conformer was less stable by 7.6 kcal/mol. Hence, only the first two conformers were considered at the second stage of optimization. The effect of solvation with THF was studied by performing additional optimizations within the polarized continuum model ($\varepsilon = 7.58$) [20] at the B3LYP/6-311G** level. Excited singlet electronic states for the most stable conformers were calculated using the time-dependent B3LYP/6-311G** method [21], with the effect of THF included by using the PCM model.

Results and Discussion

Absorption Spectra and Their Analysis on the Base of the Quantum-chemical Calculations

Figure 1(a, b, c) shows the absorption spectra of I, II and III in neat THF and its hydrochloric acid solutions at different HCl concentrations (from 0.098 to 6.065 M) keeping a constant solute concentration of 10^{-4} M. The absorption spectra, as it is seen in Fig. 1a, b and c, possess two bands: the long-wavelength band in the region of 260–340 nm and the short-wavelength band in the 210–260 nm region. In our paper the bands are signed as C and B, respectively. In
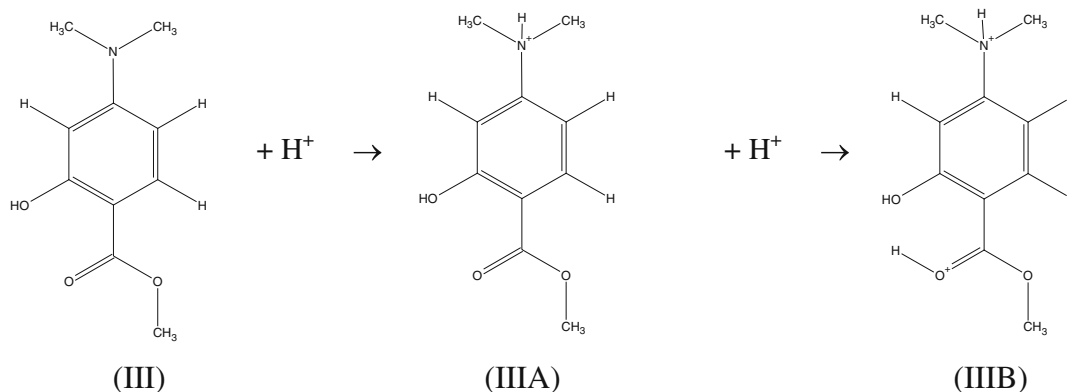
Methyl p-dimethylaminobenzoate

(I)   (IA)   (IB)
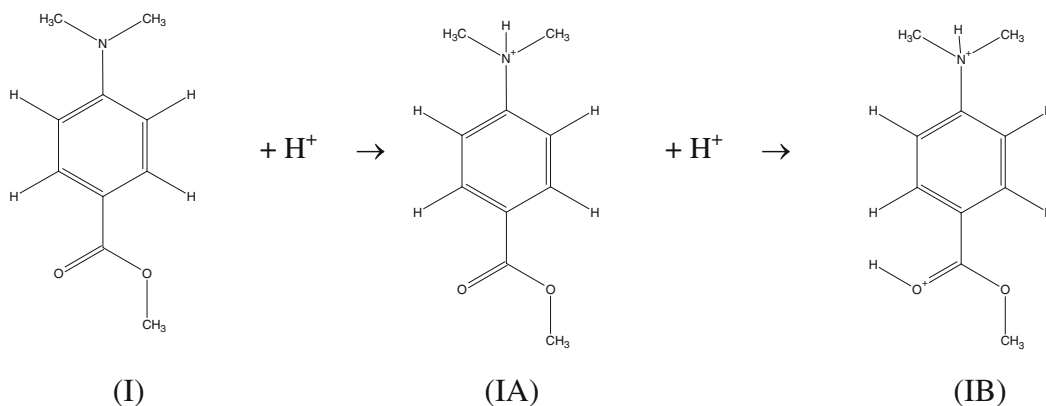
Methyl o-methoxy p-dimethylaminobenzoate

(II)   (IIA)   (IIB)

Methyl o-hydroxy p-dimethylaminobenzoate

(III)   (IIIA)   (IIIB)
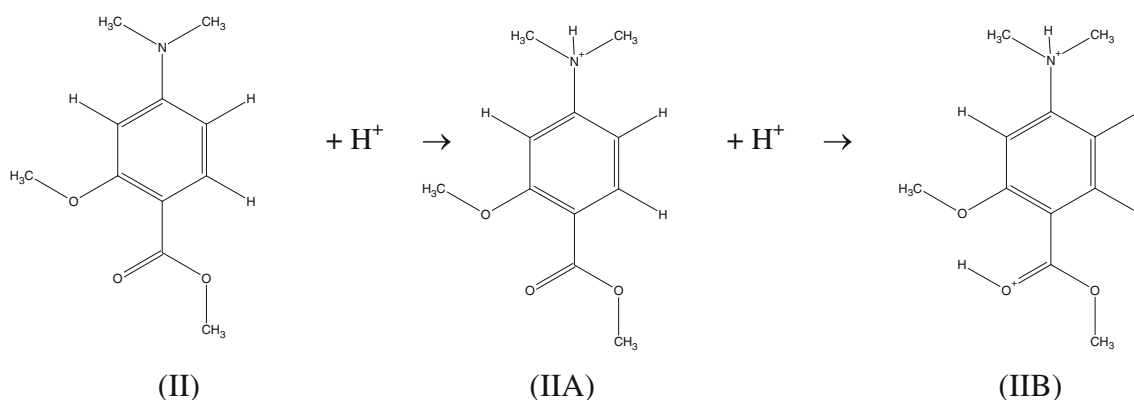
Scheme 1 Structures of methyl p-dimethylaminobenzoate and its o-methoxy and o-hydroxy derivatives (first column) and their monoprotonated (second column) and diprotonated (third column) forms

order to clarify the folded structure noted in the absorption spectrum of the molecules I, II and III, in our previous study we performed quantum-chemical calculations on these systems in vapour-phase [8]. From these calculations, it is evident that the long-wavelength absorption band in vapour-phase consists of two overlapping components (see

Fig. 1 and Table 2). It has been shown [7, 8] that the calculated $S_0 \rightarrow S_1$ transition in the studied compounds is described by the same linear combination of HOMO and LUMO one electron π-orbital transitions (only with different composition) as the S_0 (^1A) $\rightarrow$ S_1 (^1L_b) band of benzene and MB (methyl benzoate). Additionally, the strong

Table 1 Number of optimized structures and local minima for each step of conformation searches

Structure	First step (B3LYP/6-31G*)		Second step (B3LYP/6-311G**)	
	Optimized structures	Local minima	Optimized structures	Local minima
I	432	8	7	1
IA	432	12	4	2
IB	864	15	11	6
II	2592	27	6	3
IIA	179	17	9	8
IIB	329	20	2	2
III	116	12	4	2
IIIA	112	16	5	4
IIIB	218	30	2	2

peak located at 211 nm (47,400 cm^{-1}) for II and at 215 nm (46,500 cm^{-1}) for III (see Fig. 1b and c) corresponds to the allowed transitions of benzene (S_0 (^1A) $\rightarrow$ S_1 (^1B_b), signed by us as A band) at $\nu \cong 54{,}000$ cm^{-1}.

Here we would like to note that for all studied molecules in vapour-phase the longer wavelength transition possesses weaker intensity than that of the shorter wavelength (see Fig. 1 and Table 2). Its relative intensities $\left(I_{S_2}^{abs}/I_{S_1}^{abs}\right)$ depend on the molecules and equal 37 (for I), 8 (for II) and 9 for (III). In or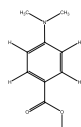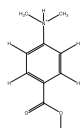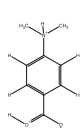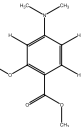der to explore the role of solute-solvent interactions, all calculations concerning absorption spectra of neutral and protonated molecules were performed in THF. It is important to note here that results of 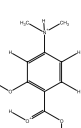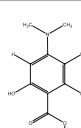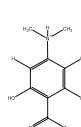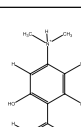quantum-chemical calculations suggest that in THF the very weak long-wavelength transition is overlapped by the red-shifted shorter wavelength transition peak. As a consequence in polar solvents long-wavelength absorption spectrum of molecules under study possesses only one transition (see Fig. 1 and Table 2). Despite the fact that the theoretical calculations suggest only one transition in the long-wavelength
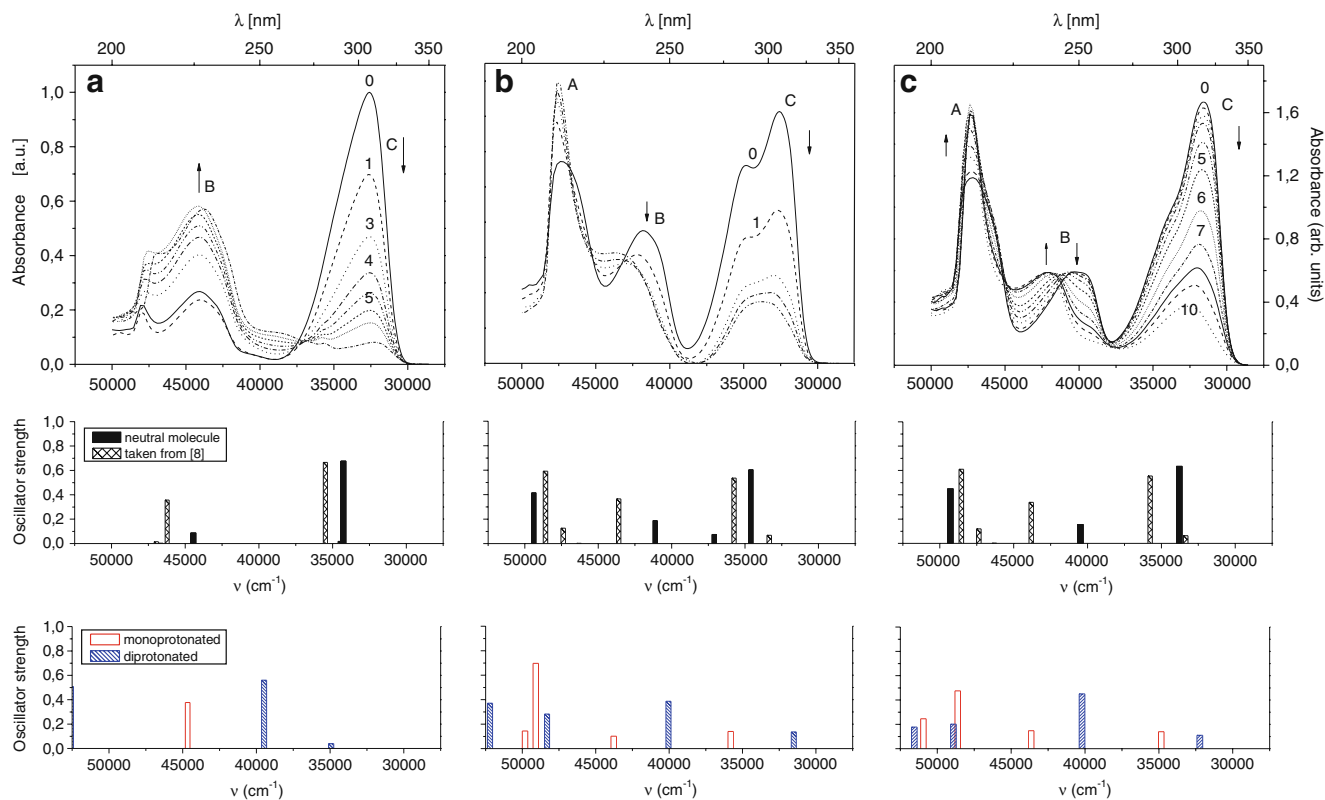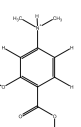
Fig. 1 Absorption spectra of I (**a**), II (**b**) and III (**c**) as a function of the HCl concentration in THF; 0-neat THF; 1–0.1 M; 2–0.2 M; 3–0.29 M; 4–0.49 M; 5–0.98 M; 6–1.97 M; 7–2.79 M; 8–3.6 M; 9–4.43 M and 10–6.065 M. The bars under the absorption curves give the theoretical electronic state energy values and corresponding oscillator strengths of neutral molecules in vapour-phase (taken from [8]) and in THF, and mono- and dicationic forms of the parent molecule in THF

Table 2 Theoretical values of singlet excited states, E_i, and corresponding oscillator strengths, f_i, of molecules under study

Compound		Transition state	E_i (cm^{-1})	f_i
I		S_1	34267,7 / 34494,7[a]	0,6764 / 0,0180[a]
		S_2	/ 35494,3[a]	/ 0,6659[a]
		S_3	44452,3 / 46227,5[a]	0,0875 / 0,3572[a]
		S_4	53259,5 / 46639,9[a]	0,2935 / 0,0022[a]
		S_5	54185,9 / 46960,2[a]	0,4138 / 0,0147[a]
IA		S_1	44664,8	0,3770
		S_2	53050,4	0,5279
		S_3	53084,2	0,3330
		S_4	54100,8	0,2414
IB		S_1	34930,8	0,0401
		S_2	39488,2	0,5601
		S_3	52590,1	0,5086
II		S_1	34602,1 / 33355,2[a]	0,6039 / 0,0680[a]
		S_2	/ 35750,3[a]	/ 0,5355[a]
		S_3	37105,8 / 43606,7[a]	0,0747 / 0,3656[a]
		S_4	41126,9 / 46306,4[a]	0,1885 / 0,0022[a]
		S_5	49385,2 / 47387,2[a]	0,4161 / 0,1262[a]
IIA		S_1	35805,1	0,1399
		S_2	43773,2	0,1019
		S_3	49079,8	0,6967
		S_4	49810,7	0,1442
IIB		S_1	31507,0	0,1367
		S_2	40048,0	0,3873
		S_3	48311,5	0,2824
		S_4	52200,2	0,3708
III		S_1	33784,9 / 33351,2[a]	0,6331 / 0,0632[a]
		S_2	/ 35761,1[a]	/ 0,5549[a]
		S_3	40480,9 / 43814,5[a]	0,1553 / 0,3381[a]
		S_4	49282,9 / 46304,7[a]	0,4491 / 0,0020[a]
IIIA		S_1	34845,6	0,1387
		S_2	43643,3	0,1473
		S_3	48614,5	0,4750
		S_4	50939,8	0,2457
IIIB		S_1	32225,8	0,1099
		S_2	40201,0	0,4508
		S_3	48911,7	0,2007
		S_4	51554,4	0,1778

[a] Theoretical values of singlet excited states, E_i, and corresponding oscillator strengths, f_i, of neutral molecules in vapour-phase are taken from [8]

absorption spectrum in THF solution the long-wavelength band consists of two transitions pictured by Gaussian profiles [7, 8], possessing maxima at 304.9 nm and 291.3 nm for I, 309.9 nm and 288.2 nm for II and 318.7 nm and 299.3 nm for III, respectively. It is important to note here that these two transitions undergo an energy-level reversal of the charge transfer and normal electronic transitions upon the environment change from vapour phase to the solvents [8, 22–24]. This phenomenon (energy-level reversal) has also been observed in the absorption spectrum of p-aminosalicylic acid and methyl p-dimethylaminobenzoate by the change of solvent from non-polar to polar one [22–24]. It must be noted that performed calculations using the Gaussian 09 code within the polarized continuum model of the solvent used do not confirm this phenomenon although the obtained absorption spectra show its existence.

As can be seen in Figs. 1 and 2, the absorption and the fluorescence spectra of molecules under study undergo very complex changes when adding HCl to the THF solution. The absorption spectra of each compound in acidic THF solutions form isobestic points, i.e., for molecule I only one is located at $\nu=37,500$ cm^{-1} (266.7 nm), for molecules II and III two points are located at $\nu=42,300$ cm^{-1} (236.4 nm) and 45,200 cm^{-1} (221.2 nm), and at 41,200 cm^{-1} (242.7 nm) and 45,000 cm^{-1} (222.2 nm), respectively. Noted changes of the absorption spectra suggest that the solute molecules undergo prototropic reactions in the electronic ground, S_0, and excited, S_1, states.

As can be seen in Fig. 1, upon increasing the HCl concentration the intensity of the C absorption band decreases. In the case of molecule I this behaviour is accompanied by the intensity increase of the B band. On the other hand, for molecules II and III new bands at $\nu \cong 44,000$ cm^{-1} (227.3 nm) (molecule II) and 42,500 cm^{-1} (235.3 nm) (molecule III) are being created (see Fig. 1). For these molecules a significant increase of the A band intensity, and a decrease of theirs full-width at half maximum, $\Delta\nu_{1/2}$, is also noticed.

In order to make the understanding the prototropic reactions appearing in the molecules under study more clear, Table 3 assembles the long-wavelength absorption and LE and ICT fluorescence bands maxima (obtained using a linear combination of Gaussian profiles, it is not shown here) of molecules in acidic solutions of THF. Analysing the assembled spectra in Fig. 1 and data collected in Table 3, we can state that:

i.   Addition of HCl acid to the neat solution generates a H$^+$ reaction with the non-bonding electrons of the –NMe$_2$ or –COOMe (–OAc) substituents of the molecules under study. The H$^+$ ion forms a chemical bond with the n-electrons of N atom of the dimethylamino substituent or with the –OAc group. In consequence, new cationic functional groups –NH$^+$Me$_2$ and

Fig. 2 Normalized fluorescence spectra of I (panels I (a) and I (a')), II (panels II (b) and II (b')) and III (panels III (c1), III (c1'), III (c2) and III (c2')) excited at different wavelengths in neat THF and for different concentrations of HCl. The concentration of HCl is: 0–0 M; 1–0.1 M; 2–0.2 M; 3–0.29 M; 4–0.49 M; 5–0.98 M; 6–1.97 M; 7–2.79 M; 8–3.6 M; 9–4.43 M and 10–6.065 M. Arrows indicate the fluorescence intensity changes caused by an increasing HCl concentration

COH$^+$OMe are formed. The –NH$^+$Me$_2$ group does not conjugate with the benzene skeleton whereas the COH$^+$OMe substituent decreases the electron accepting abilities of MB (methyl benzoate) moiety.

ii. The positions of the absorption maxima, λ_{SW}^G and λ_{LW}^G (obtained using the Peak Fit program to decompose the long-wavelength C band into a linear combination of Gaussian functions), do not change when adding HCl to the THF solution. The noticed differences in the λ_{SW}^G and λ_{LW}^G for different HCl concentrations (see Table 3) lie in the error limit of their experimental and computer fitting program determination.

To test whether the changes in the absorption spectra originate from the mono- and/or dications of the parent molecules, a series of quantum-chemical calculations were carried out. As mentioned earlier, Fig. 1 presents the absorption spectra of molecules under study as a function of the HCl concentration in THF. Additionally in the lower panels of Fig. 1, the bars under the absorption curves give the theoretical electronic state energy values and corresponding oscillator strengths of the neutral molecules in vapour-phase (taken from [8]) and in THF, and the mono- and dicationic forms of the parent molecule. Table 2 assembles the spectroscopic data (energy values of the $S_{i=1,\ldots}$ states and the associated oscillator strengths) concerning the low-lying states (up to 50,000 cm^{-1}) for the neutral molecules and their mono- and dicationic forms. Analyzing the data assembled in Table 2 in connection with the graphical presentation in Fig. 1, it follows that:

i.   The absorption spectra of molecules under study in hydrochloric acid solutions consist of electronic transitions of three different luminescent centers, absorbing at different wavelengths (i.e., neutral molecule and its mono- and dicationic forms—their formation are represented by the reactions (1), (1a) and (1b), see Chapter 3.4). Generally, the participation of protonated forms of studied molecules in absorption spectrum is higher for high concentrations of HCl. The absorption of these components contributes more at the short-wavelength at the absorption spectrum for I, whereas in the case of II and III it contributes in the long-wavelengths part, also (see Fig. 1 and Table 2).

ii. The intensity of the C absorption band decreases upon increasing the HCl concentration. The long-wavelength
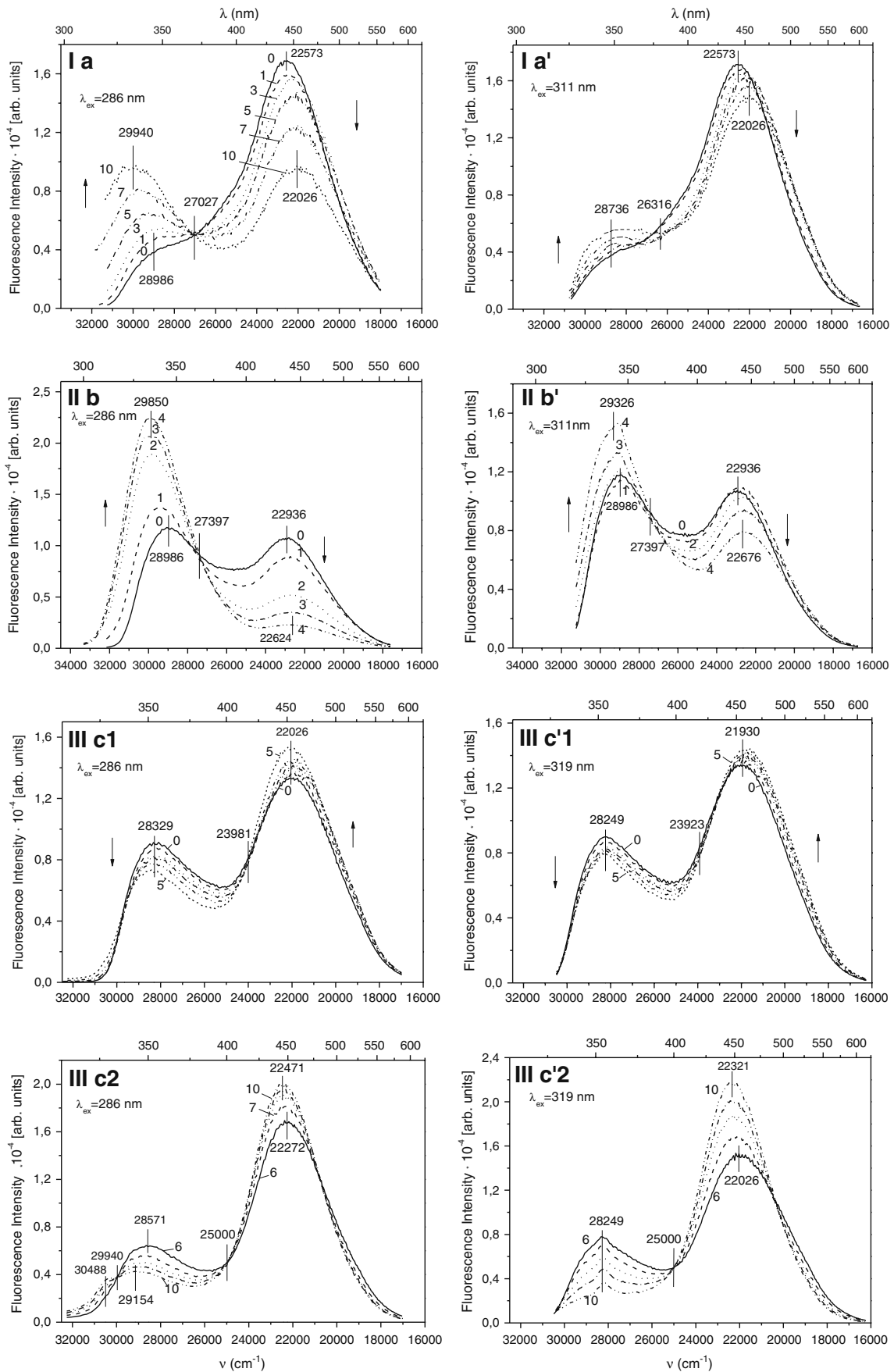
Table 3 The long-wavelength absorption and LE and ICT fluorescence bands maxima (obtained using a linear combination of Gaussian profiles) (in nm/cm^{-1}) of molecules I, II and III in acidic solutions of THF

Molecule	Long-wavelength absorption band (nm/cm^{-1})		λ_{ex} (nm)	Fluorescence band maxima (nm/cm^{-1})	
	λ_{SW}^{G} [a]	λ_{LW}^{G} [a]		λ_F (LE)	λ_F (ICT)
I					
HCl concentration 0 M					
	291.3	304.9	286/311	353.9	443.8
	34,329	32,798		28,257	22,533
HCl concentration 2.2 M					
	284.6	308.5	286	334.8	452.4
	35,133	32,420		29,868	22,104
			311	355.4	454.5
				28,137	22,004
II					
HCl concentration 0 M					
	288.2	309.9	286/311	345.0	435.7
	34,698	32,362		28,986	22,952
HCl concentration 0.39 M					
	286.3	304.9	286	335.5	441.9
	34,928	32,798		29,806	22,630
			311	342.7	443.3
				29,180	22,558
III					
HCl concentration 0 M					
	292.4	318.7	286/319	354.6	454.5
	34,203	31,377		28,201	22,002
HCl concentration 0.98 M					
	291.6	317.3	286	352.0	454.7
	34,290	31,520		28,409	21,993
			319	353.9	459.4
				28,257	21,768
HCl concentration 1.97 M					
	291.5	317.0	286	349.7	449.6
	34,300	31,550		28,600	22,244
			319	353.3	456.7
				28,303	21,879
HCl concentration 6.07 M					
	290.7	311.2	286	343.2	446.8
	34,400	32,135		29,138	22,380
			319	354.9	447.3
				28,175	22,358

[a] Determined from the decompositions of the long-wavelength absorption band into two separated Gaussian bands

absorption band in the presence of HCl at its maximum concentration used consists of two overlapping components (mono- and dicationic forms) for II and III, whereas for I, it corresponds to the $S_0 \rightarrow S_1$ transition of the dicationic form of the parent molecule (see Fig. 1 and Table 2).

iii. For molecule I, the intensity of the B absorption band increases as the HCl concentration increases. This behaviour is understandable in terms of the $S_0 \rightarrow S_1$ transition of the monocationic form of molecule I. It is important to note here that the new bands at $\nu \approx 40,000$ cm^{-1} (for I), $\nu \approx 44,000$ cm^{-1} (for II), and $\nu \approx$

42,500 cm^{-1} (for III) correspond to the $S_0 \rightarrow S_2$ transition of the dicationic form of I and of the monocationic forms of II and III, respectively.

Steady State LE and ICT Fluorescence Spectra Analysis

As it was shown in the previous section (see also Fig. 1), in acidic solutions a part of neutral solute molecules is excluded from the fluorescence emission as a result of the prototropic reaction. Figure 3 shows exemplary fluorescence spectra of III in neat THF and its hydrochloric acid solutions at different HCl concentrations. It is seen that the intensity of both (LE and TICT) fluorescence bands decreases with increasing concentration of HCl. To obtain more information about the HCl concentration effect on the both emission modes of the fluorescence spectrum of molecules under study the analyzed fluorescence spectra are normalized in a way that each of the areas under the fluorescence curves were normalized to unity. In this case, each fluorescence spectrum corresponds to the emission from the same number of emitting solute molecules under study. In the studied concentration range of HCl, the fluorescence spectra consist of two partially overlapping bands, i.e., the short-wavelength (LE) band at about 350 nm (28,571 cm^{-1}) and the long-wavelength (ICT) band at about 450 nm (22,222 cm^{-1}). Figure 2 shows that in a neat THF solution the ICT fluorescence band of I, which is assigned to the emission from the non-planar (TICT) form, dominates. In the 0–1.79 M concentration range of HCl the ratio of non-planar (TICT) to planar (LE) emitting forms (for λ_{exc}= 286 nm) changes from 81 vs. 19 to 63 vs. 37%, respectively, whereas for λ_{exc}=311 nm the ratio shows very week dependence on the HCl concentration. In the case of molecule II in the neat THF solution (see Fig. 2), the number of both

emitting forms is almost equal (52 vs. 48%). The concentration change of HCl from 0 to 0.49 M (the reaction of H$^+$ ion binding to the N or O atom of the –NMe$_2$ or –OAc substituent, respectively) causes the intensity change of both bands giving the final ratio 11 vs. 89% (for λ_{exc}=286 nm).

In the case of molecule III, (see Fig. 2), the changes of the fluorescence spectra are more complex, i.e., the fluorescence spectrum of III in a mixed solution leads to two isosbestic points, in distinction to one isosbestic point for I and II. The presence of these points indicates a formation of well defined 1:1 or 1:2 H$^+$ complexes in the emitting ensemble of molecules. The above observation is supported by respective changes in the location of the LE and ICT emission peaks maxima. In the present paper, the fluorescence behaviour of the molecules under study has been studied as a function of the excitation wavelength (i.e. the short-wavelength (λ_{exc}= 286 nm for all studied molecules) and the long-wavelength excitation ((λ_{exc}=311 nm for I, II and 319 nm for III)). It is noteworthy that for higher concentration of HCl, when excitation is carried out at the long-wavelength part of the absorption spectrum mainly neutral form of molecule I is excited, whereas in the case of molecules II and III the mono- and dicationic are excited also (see Fig. 1).

Table 3 assembles the absorption (decomposed into two Gaussian profiles) and emission peak maxima of the neutral and cationic forms of the molecules under study. A scrupulous analysis of the emission spectra determined in neat and mixed solutions (see Fig. 2 and Table 3) allows to state that:

i. When the concentration of HCl increases from 0 to the maximum concentration used and the excitation wavelength equals 286 nm the LE fluorescence band of I and II is shifted to the shorter wavelength by about

Fig. 3 Fluorescence spectra of III in neat THF and its hydrochloric acid solutions at different HCl concentrations. Insert—Stern-Volmer plots of the fluorescence quenching of III in THF using HCl as a quencher
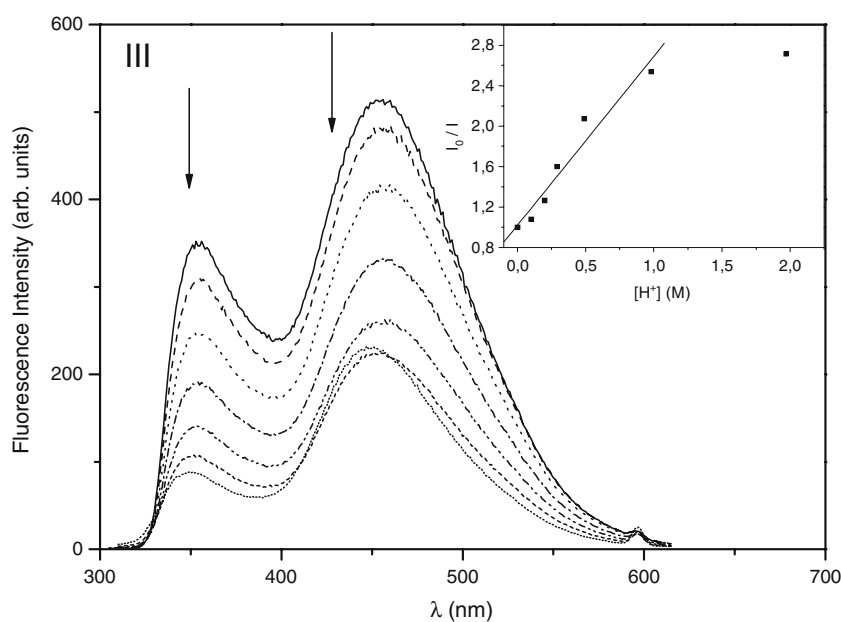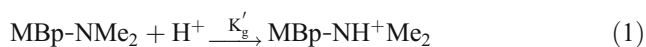
900 cm^{-1}, whereas the ICT band is shifted to longer wavelength by about 550 cm^{-1} (I) and 310 cm^{-1} (II). Upon increasing the concentration of HCl, the intensity of the LE band increases. This behaviour is accompanied by a decrease of the ICT fluorescence band.

ii. The fluorescence spectra of I and II recorded by excitation at λ_{exc}=311 nm show the same general dependences as observed for the short-wavelength excitation (λ_{exc}=286 nm).

iii. The fluorescence spectra of III will be discussed for two regions of HCl concentrations: 0–0.98 M and 1.97–6.06 M (see Fig. 2). In the first region, the emission spectra of III excited at 286 nm constitute two distinct isosbestic points at 417 nm (23,981 cm^{-1}) and 337 nm (29,674 cm^{-1}). The intensities of both bands change in an opposite direction in comparison to these of molecules I and II, i.e., the intensity of the ICT band increases whereas the LE band decreases by increasing the HCl concentration. Additionally, a new band located at $\lambda_{max} \cong 328$ nm (30,488 cm^{-1}) appears—for a low HCl concentration as a distinct tail and for higher HCl concentrations as a distinct band (see Fig. 2). It is important to note that for molecule III (λ_{exc}=319 nm) dissolved in acidic solutions in the studied concentration range of HCl the LE band position does not change whereas the ICT band is hypsochromically shifted by about 400 cm^{-1}, in comparison to the λ_{max} (ICT) value of III in the neat THF solution. The above findings point that the fluorescence of the two spatial forms (LE and TICT) of studied molecules are quenched by the H$^+$ ions differently. The next sections of this paper are devoted to the above phenomenon.
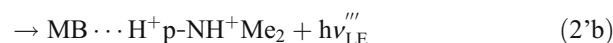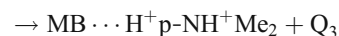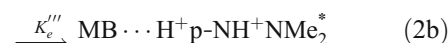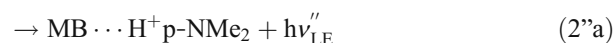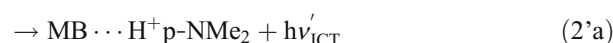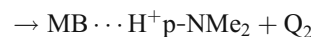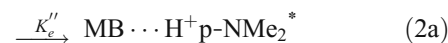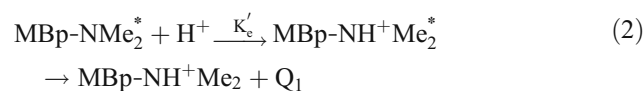
Static Studies of the H$^+$ Reaction in the S_0 and S_1 States

At it was shown earlier the steady-state absorption and emission spectra of the molecules under study in acidic THF solutions undergo complex changes, i.e., the intensity of the long-wavelength absorption band decreases and simultaneously in the UV region a new band is created. Similar changes take place in their fluorescence spectra. The isobestic points noted in the absorption and fluorescence spectra suggest a formation of complexes in the S_0 and S_1(LE) states. We suppose that between the studied molecules and the H$^+$ ion the following reactions can take place:

in the S_0 state

$$\text{MBp-NMe}_2 + \text{H}^+ \xrightarrow{K_g'} \text{MBp-NH}^+\text{Me}_2 \qquad (1)$$

$$\xrightarrow{K_g''} \text{MB}\cdots\text{H}^+\text{p-NMe}_2 \qquad (1a)$$

$$\xrightarrow{K_g'''} \text{MB}\cdots\text{H}^+\text{p-NH}^+\text{Me}_2 \qquad (1b)$$

and in the S_1 state

$$\text{MBp-NMe}_2^* + \text{H}^+ \xrightarrow{K_e'} \text{MBp-NH}^+\text{Me}_2^* \qquad (2)$$

$$\rightarrow \text{MBp-NH}^+\text{Me}_2 + Q_1$$

$$\rightarrow \text{MBp-NH}^+\text{Me}_2 + h\nu_{LE}' \qquad (2')$$

$$\xrightarrow{K_e''} \text{MB}\cdots\text{H}^+\text{p-NMe}_2^* \qquad (2a)$$

$$\rightarrow \text{MB}\cdots\text{H}^+\text{p-NMe}_2 + Q_2$$

$$\rightarrow \text{MB}\cdots\text{H}^+\text{p-NMe}_2 + h\nu_{ICT}' \qquad (2'a)$$

$$\rightarrow \text{MB}\cdots\text{H}^+\text{p-NMe}_2 + h\nu_{LE}'' \qquad (2''a)$$

$$\xrightarrow{K_e'''} \text{MB}\cdots\text{H}^+\text{p-NH}^+\text{NMe}_2^* \qquad (2b)$$

$$\rightarrow \text{MB}\cdots\text{H}^+\text{p-NH}^+\text{Me}_2 + Q_3$$

$$\rightarrow \text{MB}\cdots\text{H}^+\text{p-NH}^+\text{Me}_2 + h\nu_{LE}''' \qquad (2'b)$$

where Q_1, Q_2 and Q_3 present vibrational energies converted into heat. Naturally, the different luminescent centers (i.e., neutral molecule and its mono- and dicationic forms) absorb at different wavelengths (see Fig. 1). Also, it is important to note that light absorption can promote different luminescent centers (products of reactions (1), (1a), and (1b)).

In the first group of reactions, Eqs. 1, 1b, 2, 2', 2b and 2'b, the electron donating substituent (–NMe$_2$) of methyl benzoate (MB) is replaced by the –NH$^+$Me$_2$ group, in which the H$^+$ ion forms an ionic bond with the non-bonding n-electrons of N. The new formed substituent loses the electron donating ability and does not conjugate with the MB skeleton. This mono-cation possesses (as shown in Fig. 1 and Table 2) an absorption spectrum appearing in a different spectral region. Its spectrum is similar to the absorption spectrum of MB and its ortho derivatives [25]. The formed complex, described by reactions (1a) and (2a), (2'a), (2''a), and (2'b) possesses a chemical bond with the –OAc group, i.e.,—CO⋅⋅⋅H$^+$OMe, which does not influence the conjugation between the benzene skeleton and the acceptor moiety of these molecules. However, it must be added that the bond between benzene and the –CO⋅⋅⋅H$^+$OMe group is weakened causing a blue shift of the long-wavelength Gaussian profile of the absorption band (see Fig. 1 and Table 3). This complex emits LE

fluorescence quanta, the energies of which differ from those in the neat THF solution by 950 cm^{-1}, 860 cm^{-1} and 2,160 cm^{-1} for I, II and III, respectively. The efficiency of these reactions depends on the reaction equilibrium constant for each channel. The equilibrium constants for the formation of 1:1 complex in the S_0 state and in the S_1 state can be determined from the steady-state spectroscopic measurements using the expression proposed by Benesi and Hildebrand for absorption and fluorescence data [26, 27]:

$$\frac{1}{A - A_0} = \frac{1}{K_g(A - A_0)}\frac{1}{[H^+]} + \frac{1}{A - A_0}, \tag{3}$$

$$\frac{1}{I - I_0} = \frac{1}{K_e(I - I_0)}\frac{1}{[H^+]} + \frac{1}{I - I_0} \tag{4}$$

where A_0, A are the absorbances and I_0, I are fluorescence intensities of the neat and acidic solution and $[H^+]$ is the ion concentration. The available absorption and emission spectra do not allow determining the reaction equilibrium constant for each separate reaction channel. Thus the K_g and K_e values are resultant equilibrium constants of reactions in the ground, S_0, and excited, S_1, states, respectively.

Figure 4a and b illustrated the double reversal dependence of $1/(A-A_0)$ vs. $[H^+]^{-1}$. For each molecule, A_0 and A are the areas under the absorption profile of the long-wavelength band $\int A(\tilde{v})d\tilde{v}$ of the neat and acidic solutions of THF. As it was shown in Fig. 4 the linearity of the plots (Eq. 3) is satisfactory. The correlation coefficient being larger than 0.94 indicates a good linearity. Using the Benesi-Hildebrand equation (Eq. 3) the K_g data are determined and their values are assembled in Table 4.

Figure 5 illustrated exemplary straight lines resulting from the linear regression of the LE and ICT fluorescence data fitted to Eq. 4. The correlation coefficient being larger than 0.92 indicates good linearity. Table 4 collects the K_e^{LE} and K_e^{ICT} data determined using the Benesi-Hildebrand procedure. As it was mentioned above the K_e^{LE} and K_e^{ICT} values are resultant equilibrium constants of reactions (2'), (2''a), (2'b) and (2'a) initiated by exciting the fluorophore at λ_{SW}^G and λ_{LW}^G, respectively. Analysing the K_g and the K_e^{LE}, K_e^{ICT} data, it follows that the equilibrium constants of protopropic reactions in the S_0 and S_1 states differ for each molecule under study. The obtained data fulfil the inequalities $K_g > K_e^{LE}$ and $K_g > K_e^{ICT}$. Also, their values fulfil the following dependencies K_g (I) > K_g (II) > K_g (III) and K_e (I) > K_e (II) > K_e (III), what points that the protopropic reaction of molecules under study is most efficient for molecule I. From Eqs. 2, 2a, and 2b, it follows that these reactions are exothermic, the formed complexes are radiationless and supports fluorescence quenching phenomenon, whereas their emission (see Eqs. 2', 2''a, 2'b and 2'a)
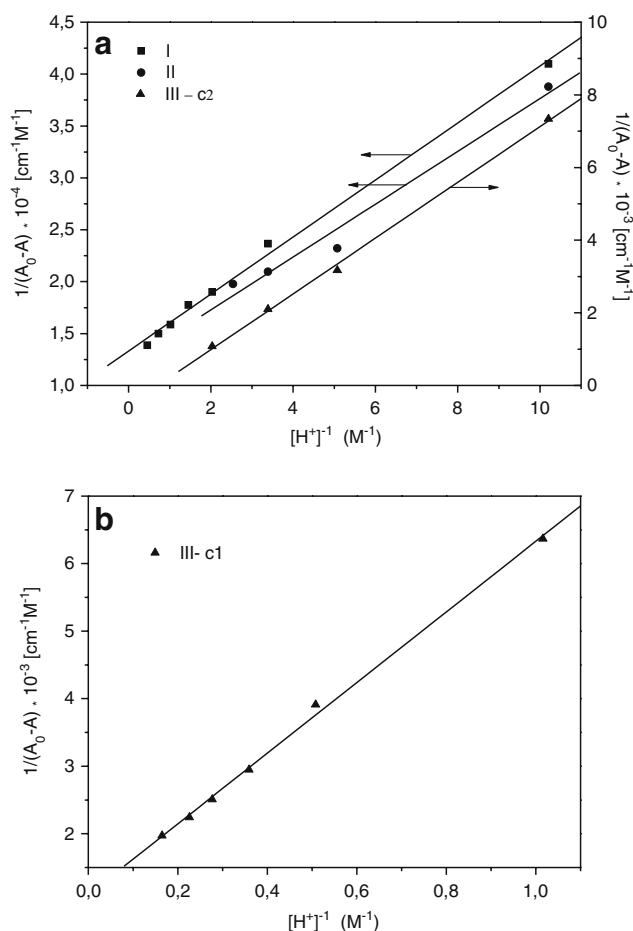
Fig. 4 The Benesi-Hildebrand dependence ($1/(A-A_0)$ vs. $[H^+]^{-1}$) for I, II and III in acidic solutions of THF. c1, c2—low and high concentration range, respectively

supplies quanta at wavelengths that are shorter than those observed for the LE fluorescence band (if the fluorophore is excited at λ_{SW} (see Table 3)) or quanta at wavelengths that are longer than those observed for the ICT fluorescence band of the neat solutions (see Figs. 1 and 2).

Analysing the K_g and K_e data collected in Table 4 in connection with the spectra pictured in Figs. 1, 2 and 3, we can state that:

i. The molecules I, II, and III show different ability to react with the H$^+$ ion. The affinities to H$^+$ also differ between the S_0, S_1(LE), and S_1(FC) states.
ii. The changes in the absorbances as well as in the LE and ICT fluorecscence band intensities are well described by the respective Benesi-Hildebrand equations.
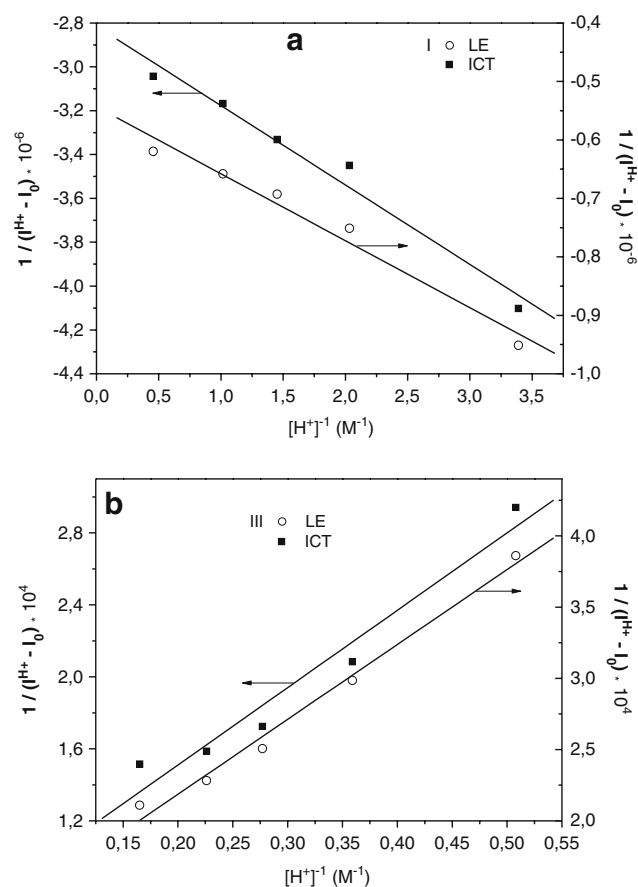iii. The K_e^{LE} and K_e^{ICT} values depend on the excitation wavelength.

Analysing the LE and ICT fluorescence intensity changes, it is evident (see Figs. 1, 2 and 3), that the prototropic reactions possess different yields for each molecule. As it was mentioned earlier, Fig. 2 shows the

Table 4 The equilibrium constants of the H+ complex formation in the ground, K_g, and excited state, K_e, determined using Benesi-Hildebrand procedure

Molecule	K_g (M^{-1})		λ_{exc} (nm)	K_e (M^{-1})	
				LE band	ICT band
I	8.90		286	4.74	6.67
			311	7.78	4.72
II	5.37		286	2.62	2.77
			311	0.67	0.18
III	c1[a]	c2[a]	286	0.51	1.10
	0.48	2.92	319	0.16	0.19

[a] c1 and c2 indicate the range of low and high HCl concentration used

variation of the normalized emission spectra (fluorescence spectrum corresponds to the emission of the same number of emitting molecules) of molecules under study. From Fig. 2, it is evident that in the case of molecules I and II, upon increasing the H+ concentration the intensity of the ICT fluorescence band decreases. This behaviour is

accompanied by an increase of the LE emission band. Above changes show an apposite direction for molecule III. It is important to note that these fluorescence intensity changes are small in comparison to those noted for I and II.

In is interesting to note that the intensity changes of fluorescence spectra described by the ratio I_{ICT}/I_{LE} or by the

Fig. 5 The Benesi-Hildebrand dependence $(1/(I_{LE}^{H^+} - I_{LE})$, $1/(I_{ICT}^{H^+} - I_{ICT})$ vs. $[H^+]^{-1})$ for I—panel (**a**) and III—panel (**b**) in acidic solutions of THF
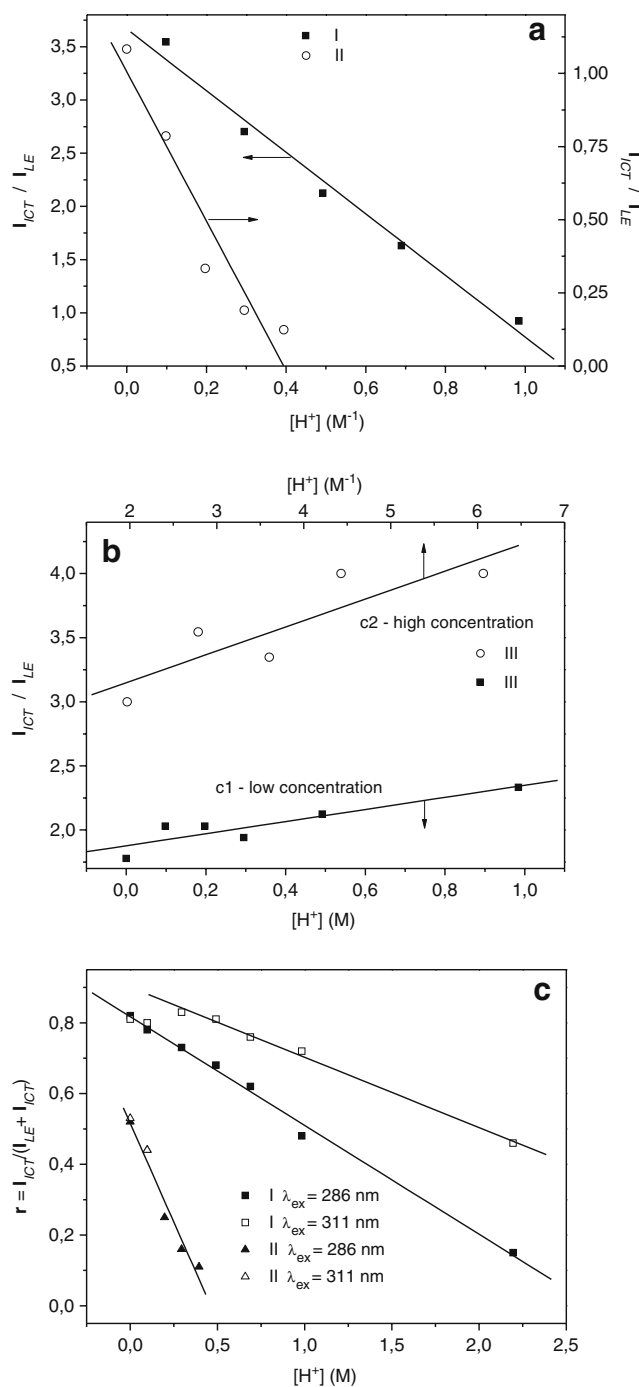
Fig. 6 Fluorescence intensity ratio I_{ICT}/I_{LE} vs. $[H^+]$ of I, II and III (panel **a** and **b**) and the ICT fluorescence band contribution coefficient, $r = I_{ICT}/(I_{LE} + I_{ICT})$ vs. $[H^+]$ (panel **c**) of I and II determined for two excitation wavelengths

coefficient of the ICT fluorescence band contribution $r = I_{ICT}/(I_{ICT} + I_{LE})$ show a linear dependence on the H$^+$ concentration (see Fig. 6). The correlation coefficient being larger than 0.94 indicates a good linearity. As can be seen in Fig. 6 the fluorescence intensity ratio I_{LE}/I_{ICT} as well as r data are very sensitive to H$^+$ concentration for I and II. These findings predestine molecules I and II to be used as acid fluorescence probes in a region of 0–2.5 M. For III these intensity changes are small, are in the error limit of their determination.

Fluorescence Quenching Caused by Photoinduced Reaction of H$^+$

Figure 3 shows the fluorescence spectra of III obtained in THF, in the presence of the HCl at its various concentrations as an example. The spectra have been obtained at fixed solute concentration ($c = 10^{-4}$ M) and for the HCl, which concentration changes from 0 to 1.97 M. As can be seen in Fig. 3, the increase of HCl concentration results in a strong decrease of the short- (LE) and long-wavelength (TICT) fluorescence bands. It is important to note here that the intensity of both fluorescence modes decreases with increasing concentration of HCl for the all studied molecules (dependence for I and II is not shown here).

It is well known that for ideal bimolecular quenching process, the Stern-Volmer equations can be applied [28, 29]:

$$I_F^0/I_F = 1 + k_q \tau_F^0 [Q] = 1 + K_{SV}[Q], \tag{5}$$

and

$$\tau_F^0/\tau_F = 1 + k_q \tau_F^0 [Q] = 1 + K_{SV}[Q], \tag{6}$$

where k_q is the bimolecular quenching constant, I_F^0 and τ_F^0 are the fluorescence intensity and lifetime in the absence of quencher. I_F and τ_F are the equivalent parameters in presence of the quencher at a concentration [Q]. If only dynamic quenching is operative without any static quenching, the K_{SV} values obtained from Eqs. 2 and 3 should be identical [28, 29].

The insert in Fig. 3 shows straight line from the plot of the I_0/I versus HCl concentration only at low quencher concentrations. Similar behavior is observed for I and II. Taking this into account, it can be concluded that the fluorescence quenching of the molecule under study in acidic THF solutions is very complex and a simple bimolecular process of the Stern-Volmer type is not sufficient to describe the noted changes in the fluorescence intensities.

Concluding the above findings, it must be stated that in a hydrochloric acid solution the studied molecules exist as a mixture of neutral, mono-, and dicationic forms. The reaction of H$^+$ with the neutral excited molecules under study creates emissive and/or non-emissive complexes. They arise in a

reaction of H$^+$ with the –OAc or/and –NMe$_2$ substituents creating mono- or/and dications of the parent molecule. Naturally, the neutral, mono-, and dicationic forms of the molecules under study possess own characteristic absorption and fluorescence spectra. Their characteristics need further detailed study using time-resolved measurements.

References

1. Gormin D, Kasha M (1988) Chem Phys Lett 153:574
2. Gormin D, Heldt J, Kasha M (1989) Chem Phys 136:321
3. Gormin D (1989) J Phys Chem 93:5979
4. Heldt JR, Gormin D, Kubicki A, Heldt J (1997) Słup Prace Mat-Przyr 11a:3
5. Aleksiejew M, Heldt JR (2007) J Lumin 126:665
6. Aleksiejew M, Józefowicz M, Heldt JR (2005) Z Naturforsch 60a:655
7. Aleksiejew M, Heldt J, Heldt JR (2008) J Lumin 128:1307
8. Aleksiejew M, Heldt J, Heldt JR (2009) J Lumin 129:208
9. Aleksiejew M (2008) Ph.D. dissertation, University of Gdańsk
10. Krishnamvorthy G, Dogra S (2000) J Phys Chem A 104:2542
11. Ghosh S, Chakraborty A, Kar S, Guchhait N (2009) J Lumin 129:482
12. Angulo G, Grampp G, Rosspeintner A (2006) Spectrochim Acta A 65:727
13. Frisch MJ, Trucks GW, Schlegel HB, Scuseria GE, Robb MA, Cheeseman JR, Scalmani G, Barone V, Mennucci B, Petersson GA, Nakatsuji H, Caricato M, Li X, Hratchian HP, Izmaylov AF, Bloino J, Zheng G, Sonnenberg JL, Hada M, Ehara M, Toyota K, Fukuda R, Hasegawa J, Ishida M, Nakajima T, Honda Y, Kitao O, Nakai H, Vreven T, Montgomery JA Jr, Peralta JE, Ogliaro F, Bearpark M, Heyd JJ, Brothers E, Kudin KN, Staroverov VN, Kobayashi R, Normand J, Raghavachari K, Rendell A, Burant JC, Iyengar SS, Tomasi J, Cossi M, Rega N, Millam JM, Klene M, Knox JE, Cross JB, Bakken V, Adamo C, Jaramillo J, Gomperts R, Stratmann RE, Yazyev O, Austin AJ, Cammi R, Pomelli C, Ochterski JW, Martin RL, Morokuma K, Zakrzewski VG, Voth GA, Salvador P, Dannenberg JJ, Dapprich S, Daniels AD, Farkas Ö, Foresman JB, Ortiz JV, Cioslowski J, Fox DJ (2009) Gaussian 09, revision A1. Gaussian, Inc., Wallingford
14. SSC: a tool for constructing libraries for systematic screening of conformers, available at http://sscf.sf.net
15. Ling S, Gutowski M (2011) J Comp Chem (under review)
16. Lee C, Yang W, Parr RG (1988) Phys Rev B 37:785
17. Stephens PJ, Devlin FJ, Chabalowski CF, Frisch MJ (1994) J Phys Chem 98:1623
18. Hehre WJ, Ditchfield R, Pople JA (1972) J Chem Phys 56:2257
19. Krishnan R, Binkley JS, Seeger R, Pople JA (1980) J Chem Phys 72:50
20. Barone V, Cossi M, Tomasi J (1997) J Chem Phys 107:3210
21. Stratmann RE, Scuseria GE, Frisch MJ (1998) J Chem Phys 109:8218
22. Shabestary N, El-Bayoumi MA (1984) Chem Phys Lett 106:107

23. Steward JJP (1983) J Com Chem 10:209
24. Parusel ABJ, Köhler G, Grimme S (1998) J Phys Chem A 102:6297
25. Sinha HK, Muralidharan SM, Yates K (1992) Can J Chem 70:1932
26. Benesi HA, Hildebrand JH (1949) J Am Chem Soc 71:2703
27. Lin L-R, Yang W-L, Zheng G-L, Tiang Y-B (2004) Spectrochim Acta A 60:2209
28. Valeur B (2002) Molecular fluorescence: principles and applications, chap 4. Wiley-VCH, Weinheim
29. Lakowicz JR (2006) Principles of fluorescence spectroscopy. Kluwer Academic/Plenum Publishing Corporation, New York